Deletions into an NH_2-Terminal Hydrophobic Domain Result in Secretion of Rotavirus VP7, a Resident Endoplasmic Reticulum Membrane Glycoprotein

MARIANNE S. PORUCHYNSKY,* CHIARA TYNDALL,‡ GERALD W. BOTH,‡ FUMIYASU SATO,§ A. RICHARD BELLAMY,§ and PAUL H. ATKINSON*

Department of Developmental Biology and Cancer, Albert Einstein College of Medicine, Bronx, New York 10461; ‡Division of Molecular Biology, Commonwealth Scientific and Industrial Research Organization, North Ryde, Australia; and §Department of Cell Biology, University of Auckland, Private Bag, Auckland, New Zealand.

ABSTRACT Rotavirus, a non-enveloped reovirus, buds into the rough endoplasmic reticulum and transiently acquires a membrane. The structural glycoprotein, VP7, a 38-kD integral membrane protein of the endoplasmic reticulum (ER), presumably transfers to virus in this process. The gene for VP7 potentially encodes a protein of 326 amino acids which has two tandem hydrophobic domains at the NH_2-terminal, each preceded by an in-frame ATG codon.

A series of deletion mutants constructed from a full-length cDNA clone of the Simian 11 rotavirus VP7 gene were expressed in COS 7 cells. Products from wild-type, and mutants which did not affect the second hydrophobic domain of VP7, were localized by immunofluorescence to elements of the ER only. However, deletions affecting the second hydrophobic domain (mutants 42–61, 43–61, 47–61) showed immunofluorescent localization of VP7 which coincided with that of wheat germ agglutinin, indicating transport to the Golgi apparatus. Immunoprecipitable wild-type protein, or an altered protein lacking the first hydrophobic sequence, remained intracellular and endo-β-*N*-acetylglucosaminidase H sensitive. In contrast, products of mutants 42–61, 43–61, and 47–61 were transported from the ER, and secreted. Glycosylation of the secreted molecules was inhibited by tunicamycin, resistant to endo-β-*N*-acetylglucosaminidase H digestion and therefore of the *N*-linked complex type. An unglycosylated version of VP7 was also secreted. We suggest that the second hydrophobic domain contributes to a positive signal for ER location and a membrane anchor function. Secretion of the mutant glycoprotein implies that transport can be constitutive with the destination being dictated by an overriding compartmentalization signal.

The targeting and sorting of membrane proteins to their different subcellular compartments has become a major topic of interest in cell biology and a problem that has become increasingly amenable to manipulation by gene cloning techniques. Membrane maturing viruses have long been used to probe questions of this nature (22) because of the high abundance of the membrane proteins of interest in infected cells. Several laboratories have used the cloned genes of membrane glycoproteins, such as influenza hemagglutinin (11, 17, 35, 38), vesicular stomatitis virus G protein (15, 19, 34), Semliki forest virus (16, 23), and rous sarcoma virus (45) to probe for the portions of the expressed products that are important in determining their plasma membrane localization. These membrane glycoproteins are characterized by a COOH-terminal hydrophobic membrane anchoring segment and a cytoplasmic tail. Disruption of the former has generally resulted in complete secretion of these molecules, which in their native state traverse most of the secretory pathway. Alterations of the COOH-terminal cytoplasmic tail had diverse effects. Some mutant proteins became blocked along the secretory pathway and others failed to traverse the pathway at all. The exact nature of the signal for targeting these proteins to the plasma

membrane was not clear from these studies. Failure of these molecules to move along the exocytosis pathway may have been due to the alteration of a positive plasma membrane targeting signal or to denaturation of the protein product.

Rotavirus VP7 is a glycoprotein of particular interest as a potential model for the study of protein transport (21). This protein associates with viral cores that bud into the lumen of the rough endoplasmic reticulum (RER)[1] (1) from cytoplasmic structures, called viroplasms. Mature virus remains within the lumen of the RER until release by cell lysis. VP7 is an integral membrane glycoprotein with a lumenal orientation (21) and is located in the endoplasmic reticulum (ER) (10, 32). The Golgi apparatus is not involved in processing the mature form of VP7, a fact confirmed by the presence on the molecule of the high-mannose form of carbohydrate (9). VP7 therefore constitutes an example of a membrane glycoprotein that is targeted to the ER and is not subsequently directed further along the secretory pathway. The cloning and sequencing of the SA11 VP7 gene revealed the presence of two tandem NH_2-terminal hydrophobic domains in the protein, and the absence of a COOH-terminal hydrophobic domain (7). Each of the hydrophobic domains is preceded by an AUG codon and could ostensibly serve as a signal peptide for the translocation of VP7, depending on which codon is read for initiation. However, the specific role of each of these codons and hydrophobic segments in VP7 synthesis is not clear. In studying the function of the hydrophobic domains, we constructed a series of deletions in the VP7 gene. Three mutants were obtained for which the VP7 proteins acquired complex carbohydrate, as distinct from the high-mannose type exhibited by wild-type VP7, showing that they traversed the secretory pathway and reached the Golgi apparatus. These proteins were also secreted. A priori, the transport of VP7 to more distal locations along the secretory route should require either the modification of a positive signal specifying ER location, or alternatively, the addition of a signal enabling vectorial transport to occur. The induction of VP7 secretion by creating various deletions in the protein is more easily explained by the disruption of a positive signal specifying ER location. We conclude that there must be a positive signal for retention of a protein in the ER. Since wild-type VP7 is naive to the secretory pathway, it is also implied that in the absence of overriding sorting signals, secretion is constitutive.

MATERIALS AND METHODS

cDNA Cloning and Construction of a Plasmid for VP7 Expression: Standard molecular cloning techniques were used in this work (29). The complete sequence of genomic segment nine of Simian 11 rotavirus was obtained previously using a partial length cDNA clone that lacked 5′-terminal sequences (7). A full-length clone was isolated using a modified cloning strategy (20). This yielded a VP7 clone inserted in the Pst I site of pBR322 which was confirmed as full length by terminal sequence analysis (30). The insert was excised with Pst I, digested with nuclease Bal 31 to remove G:C homopolymer tails, and the blunt-ended molecule was flanked with Xho I sites by the addition of phosphorylated Xho I linkers (P-L Biochemicals). The VP7 gene with Xho I termini was then inserted into the unique Xho I site of pJC119 (36) to yield plasmid pJC16 which contained the rotavirus VP7 sequence in the correct orientation downstream from the SV40 late promoter. pJC119 was obtained from by Dr. J. Condra, Division of Virus and Cell Biology Research, Merck, Sharp & Dohme Research Laboratories, West Point, PA. Sequencing revealed that pJC16 nevertheless contained residual homopolymeric sequences (15G residues) at the 5′-end of the gene. These were removed by replacing the 5′-terminal region of the clone proximal to the Nco I site with a fragment that lacked the residual homopolymeric tail. An Aha III-Nco I fragment was prepared from the SA11 VP7 clone, Xho I linkers were added to the Aha III end, and after recutting, the Xho I-Nco I fragment was cloned into the SV40 vector to generate the plasmid pJC9 (Fig. 1).

Preparation of Deletion Mutants of VP7: pJC9 was cut with Bam H1 and the 387-bp 5′-terminal fragment of the VP7 gene (Fig. 1) was subcloned into the Bam H1 site of pBR322 to generate pBR9B (Fig. 1) which contains a unique Nco I site. The plasmid was made linear by cutting with Nco I and digested with Bal 31 to remove nucleotides progressively. The products were made blunt ended, Nco I linkers (a generous gift of Dr. R. Gregson, Biotechnology Australia, Proprietary Ltd., Roseville, NSW) were added and the plasmids were religated to generate a series of deleted variants of pBR9B. These were sequenced from the Nco I site in order to identify those carrying appropriate in-frame deletions. The small Xho I/Nco I fragments containing modified 5′-regions of the gene were retrieved and incorporated into the expression vector (pJC9) by a three-way ligation as outlined in Fig. 1. Another mutant (1–14), which deleted the first ATG and therefore the first hydrophobic domain, was prepared as follows. Xho I linkers were added to an Eco RV/Bam H1 fragment (Figs. 1 and 2). This fragment was cut with Xho I and Nco I and the smaller Xho I/Nco I fragment isolated. This segment was then reincorporated into pJC9 by the three-way ligation method described above. Mutant 2–8 was constructed as follows. The oligonucleotides 5′ CATGGTTCTAACCTTTCTGATAT 3′ and 5′CGATATCAGAAAGGTTAGAAC 3′ were made using a DNA synthesizer (Applied Biosystems, Inc., Foster City, CA). These are complementary and create Nco I- and Cla I-compatible termini when annealed. The oligonucleotides were phosphorylated and ligated with the EcoR1/Xho I fragment from pJC9 (Fig. 1) and a fragment from the same plasmid, which extended through the VP7 gene, counterclockwise from the EcoR I site to the Cla I site near the 5′-end of the gene (7). The fourth fragment which permitted the vector to circularize was an Xho I/Nco I fragment of 53 bases derived from a pBR9B deletion mutant (Fig. 1), where the Bal 31 digestion went precisely to the first ATG codon. This construction deleted the first eight amino acids of VP7 which are conserved between human, simian, and bovine rotaviruses, and substituted Met-Ala-Met such that the final NH_2-terminal sequence now reads as Met-Ala-Met-Val-Leu-Thr .....

Polyclonal Anti-VP7 Antiserum: SA11 rotavirus was propagated and purified by published procedures (37). Intact double-shelled virions labeled with ^{125}I (26) were concentrated by ultracentrifugation and disrupted by boiling in an SDS dissociation buffer containing 2-mercaptoethanol (25). Viral polypeptides were resolved by electrophoresis on discontinuous slab gels (25) and the band corresponding to VP7 located by radioautography. The region of the gel containing the SDS-denatured VP7 was recovered, homogenized with incomplete Freund's adjuvant, and injected subcutaneously into rabbits. Animals were boosted at 4-wk intevals and the antiserum confirmed as monospecific by Western blot analysis (42).

Cell Growth, Transfection, Tunicamycin Treatment, and Radiolabeling: The RR1 strain of *Escherichia coli* was used for the propagation of all plasmid DNA used for transfections. After standard bacterial lysis procedures (29), DNA was isolated and purified by cesium chloride–ethidium bromide ultracentrifugation followed by precipitation and resuspension in water. The procedure for transfection of COS 7 cells (18) follows that of published procedures (34) with several modifications. COS 7 cells were grown on 100-mm dishes in Dulbecco's modified Eagle's medium (DME) (Gibco Laboratories, Grand Island, NY), containing 5% each of calf and fetal calf serum, 100 U/ml penicillin, 100 μg/ml streptomycin (Gibco Laboratories) and 2 mM L-glutamine. Monolayers that were 60–80% confluent were washed and transfected in Tris-buffered saline (19). DNA (15–30 μg/ml) was added to each plate followed by the addition of DEAE–dextran (Pharmacia Fine Chemicals, Piscataway, NJ; 2×10^6 daltons; 500 μg/ml) (19). After 1.5–2 h at 37°C, the Tris-buffered saline solution was removed and DME, containing serum as above and 100 μM chloroquine (Sigma Chemical Co., St. Louis, MO), was added to the cells. After incubation for 3 h at 37°C, DME without chloroquine but containing serum and additions as above was added. At 45 h after DNA/DEAE–dextran removal, the cells were incubated at 37°C for 1 h in DME salts lacking serum and methionine but supplemented with all other amino acids and 1 mg/ml glucose. Transfected cells were then labeled for 2.5 or 4 h at 37°C on a rocker platform in the above medium to which L-[^{35}S]methionine at a concentration of 150 μCi/ml was added. At the end of the labeling period, the medium was collected and non-adherent cells were pelleted by centrifugation in an Eppendorf centrifuge for 10 min. Supernatants were removed and analyzed for expressed secreted material.

For those cells treated with tunicamycin, dishes were incubated in medium containing tunicamycin (Sigma Chemical Co.), at a final concentration of 2

[1] *Abbreviations used in this paper:* DME, Dulbecco's modified Eagle's medium; endo-H, endo-β-*N*-acetylglucosaminidase H; ER, endoplasmic reticulum; PAS, protein A–conjugated Sepharose CL4B; RER, rough endoplasmic reticulum; R-WGA, wheat germ agglutinin conjugated to rhodamine.

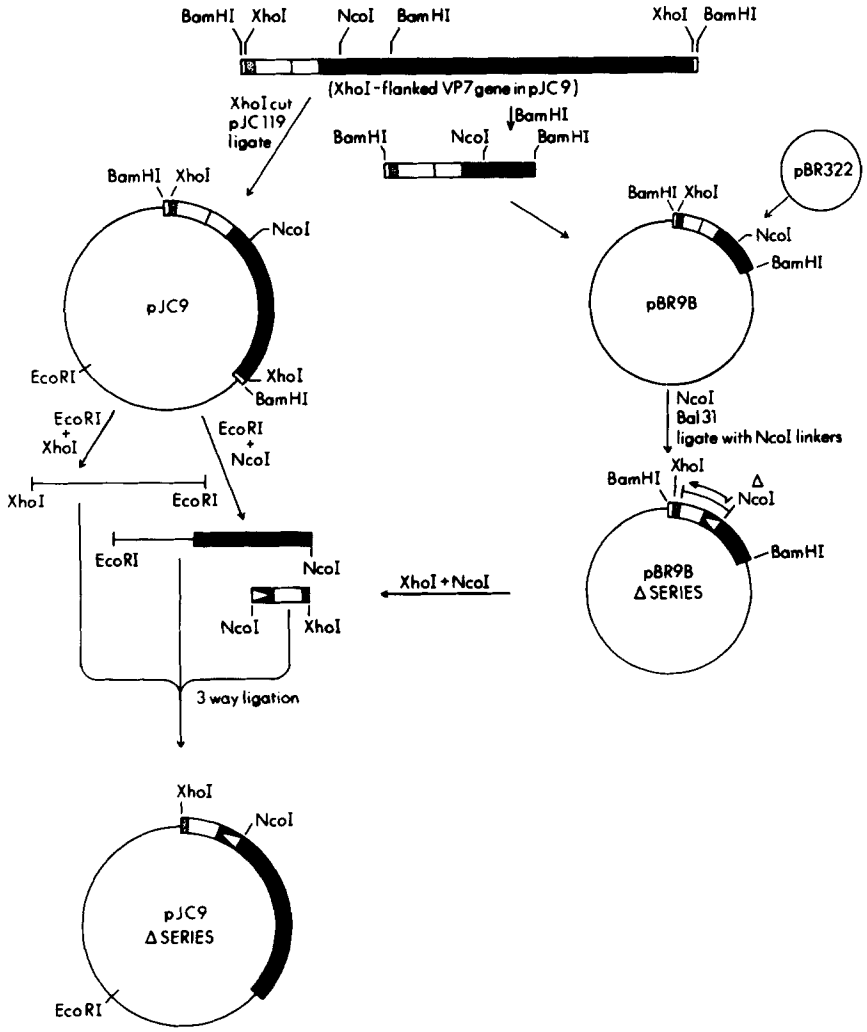

FIGURE 1 Strategy for the construction of VP7 gene deletions in an SV40 expression vector. See Materials and Methods for details. Solid bars are VP7 coding sequences. Open bars represent the location of VP7 hydrophobic domains. Thin lines are pBR322 and SV40 sequences. Stippled area corresponds to the 50-bp noncoding region of the VP7 gene 5′ to the ATG start codon.

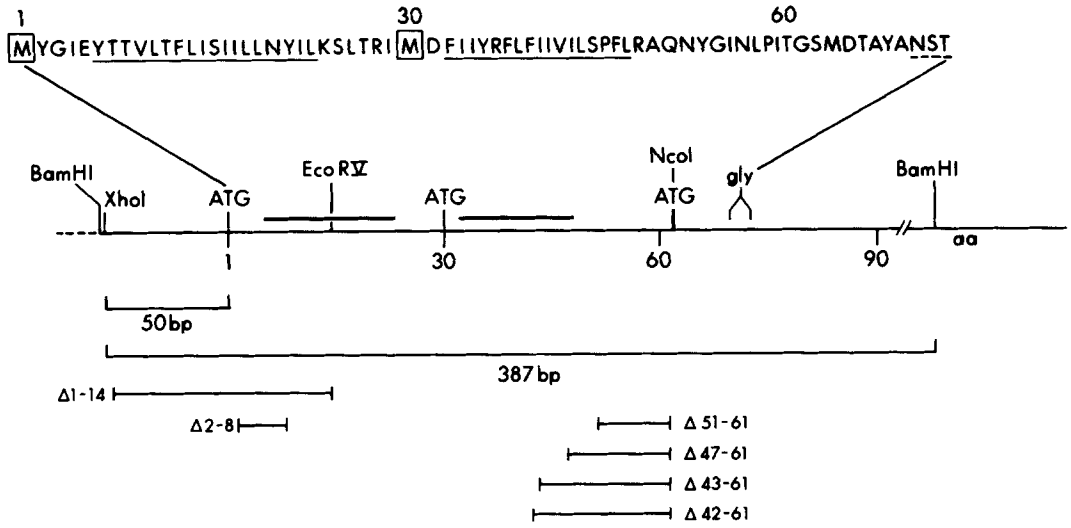

FIGURE 2 Structure of the 5′-end of the VP7 gene showing the location of deletion mutants within it and the NH_2-terminal sequence of the protein. The hydrophobic domains underlined in the amino acid sequence were identified previously (7, 9) but may vary if other criteria are applied. The single glycosylation site is located at residue 69. The deletions are numbered according to the amino acid residues actually deleted. Due to the addition of Nco I linkers in the constructions (see Materials and Methods), Ser at position 61 is changed to Ala in all mutants numbered N-61. In the complete VP7 clone used for these studies, two conservative amino acid changes occurred compared with the originally published sequence derived from an incomplete clone (7). C_{32} and L_{37} are both changed to F.

μg/ml (41), beginning at 42.5 h after transfection and continuing for 8 h thereafter. Tunicamycin was therefore present for 4 h prior to radiolabeling, including the 1-h preincubation in medium lacking methionine, as well as during the 4-h labeling period.

Immunoprecipitation: Cell monolayers were rinsed in ice-cold phosphate buffered saline (PBS), harvested, and lysed in buffer containing 1% each of deoxycholate and Triton X-100, 0.1% SDS, and 0.15 M NaCl in 25 mM Tris-HCl, pH 8.0, containing 100 U/ml Traysylol. The nuclei were pelleted (34) after the addition of more detergent. Standard procedures (3), with some modification, were used for immunoprecipitation of proteins from the postnuclear supernatant by rabbit polyclonal antiserum to VP7 and protein A–conjugated Sepharose CL4B (PAS) (Pharmacia Fine Chemicals). Beads were swollen in distilled water and added to transfected cell lysates before incubation with antibody. PAS beads were pelleted by centrifugation and discarded (12) in an attempt to eliminate any nonspecifically adherent proteins. Polyclonal anti-VP7 serum was then added to lysates which were incubated at 4°C overnight before the addition of PAS beads. These had been preincubated for several hours in a solution containing 10 mg/ml bovine serum albumin and a postnuclear cell lysate of unlabeled, untransfected COS 7 cells.

Medium from the transfected cell cultures had an equal volume of 2× lysis buffer added which contained 1 mM methionine and 1 mg/ml bovine serum albumin. Rabbit polyclonal anti-VP7 antiserum was added to each and incubated overnight at 4°C, followed by the addition of pre-absorbed PAS beads. In an effort to reduce background bands from the media in other experiments, such as that examining the effect of tunicamycin, PAS beads were additionally pre-absorbed with media from COS 7 cell cultures. Beads were pelleted from all samples and washed extensively in buffers containing detergent and then in PBS (3). After boiling the beads in 0.05 M Tris-HCl, pH 6.7, containing 1% SDS (34) to remove the bound antibody–protein complexes, 0.2 M citrate-phosphate buffer, pH 5.0, was added prior to treatment of half of each sample with 0.041 U of endo-β-*N*-acetylglucosaminidase H (endo-H) prepared as described (39), at 37°C for 1 h. A lysate of L-[^{35}S]methionine–labeled SA11-infected MA104 cells was prepared and treated with endo-H for use as a marker. The reactions were stopped by addition of buffer containing 100 mM Tris, 5% SDS, 1 mM EDTA, 50 mM dithiothreitol, 10% glycerol, 0.1% bromophenol blue, 100 μg/ml soybean trypsin inhibitor, 200 U/ml Traysylol, 5 mM β-aminocaproic acid, 1 mM benzamidine, and 2 mM phenylmethylsulfonyl fluoride. Samples were boiled for 3 min and analyzed by SDS PAGE on 12% gels (25) run at constant voltage. Gels were fixed, fluorographed in Amplify (Amersham Corp., Arlington Heights, IL) for 20 min, dried, and then autoradiographed at −70°C using Kodak SB 5 film. Composites of photographs of gels were always assembled from equivalent or identical exposures with comparable markers.

Immunofluorescent Localization and Electron Microscopy: COS 7 cells which had been grown to semi-confluency on glass coverslips (Corning Glass Works, Corning, NY), in 35-mm dishes, were transfected in Tris-buffered saline as described above, washed with chloroquine for 3 h, and incubated with DME containing serum. At 47 h after removal of DNA/DEAE–dextran, cells were washed in PBS and fixed for 45 min at 22°C in 2% formaldehyde, freshly prepared from paraformaldehyde, and then buffered in 0.05 M phosphate, pH 7.5. The coverslips were rinsed in PBS for 20 min, then soaked in 1% Triton X-100 in PBS for 20 min to permeabilize the cells. After two 10-min rinses in PBS, the coverslips were incubated for 1 h at 37°C in a solution containing polyclonal rabbit anti-VP7 diluted 1:400 in PBS and rhodamine conjugated to wheat germ agglutinin (R-WGA) (Vector Laboratories, Inc., Burlingame, CA) diluted 1:300 or 1:400. The cells were then rinsed exhaustively in PBS and incubated in a 1:300 dilution of secondary goat anti-rabbit IgG conjugated to fluorescein (Cappel Laboratories, Cochranville, PA) for 45 min at 37°C. Cells were photographed in the same plane of focus, with a Zeiss III RS photomicroscope, using appropriate filters for fluorescein or rhodamine.

To examine the ultrastructural morphology of untreated COS 7- and of SA11-infected MA104 cells (5.5 h post-infection, infected according to published methods [12]), coverslips were fixed in 2% glutataldehyde in 0.1 M cacodylate buffer, pH 7.4, for 45 min at 22°C. Cells were postfixed in 1% osmium tetroxide in cacodylate buffer, stained in 1% uranyl acetate, dehydrated in ethanol, and embedded in resin before thin sectioning. Sections were stained with uranyl rinse and Reynolds lead stain for several minutes (33) and then specimens were examined and photographed in a JEOL 100 CX electron microscope at 80 kV.

RESULTS

Morphogenesis of Rotavirus Particles in SA11-infected MA104 Cells

One novel feature of the rotavirus system is that the virus appears to be located primarily in elements of the ER (1). However, these earlier studies also showed that at 16–24 h post-infection, virus was sporadically present in other cellular organelles in cells showing extensive damage. We have examined the distribution of virus particles in cells early in infection. At 5.5 h post-infection, virus particles were found only in the ER (Fig. 3); none were ever seen in the Golgi apparatus or in mitochondria. The viroplasm structures immediately adjacent to the RER were also evident and viral cores could be seen budding from the periphery of the viroplasm into the lumen of the RER. The envelope acquired from the RER membrane was subsequently lost and both enveloped and mature virions were visible in the lumenal space (Fig. 3). VP7 has been located to the ER by immunoelectron microscopy (10, 32). In vitro translation studies have also shown it to be an integral membrane protein (21). Since the VP7 protein is found in mature virions and has only high-mannose oligosaccharides (9), the data collectively show that VP7 remains in the ER after translation. However, the mechanism by which VP7 is incorporated into the virus remains unknown. Thus, the rotavirus VP7 provides an opportunity to study the factors controlling the specific localization of proteins to the ER.

Ultrastructural Morphology of COS 7 Cells

To accurately interpret the localization of expressed VP7 protein products within COS 7 cells, it was necessary to examine the ultrastructural morphology and interrelationships of organelles in COS 7 cells, especially in the perinuclear region. These cells are characterized at their periphery by predominantly free polysomes crowding the cytoplasm and by numerous microvilli projecting from their cell surface (Fig. 4). The cells are often multinucleate, have many lipid droplets, mitochondria, and a preponderance of organelles situated close to each other around the nucleus at the center of the cell (Fig. 4, *a* and *b*). The perinuclear region is occupied by extensive branching ER, which contains numerous areas of transitional elements (Fig. 4 and *inset*) and smooth ER that spatially intertwine with, but are distinct from, the extensive perinuclear Golgi apparatus. It is evident that portions of the Golgi apparatus can surround concentrated elements of the ER.

Immunofluorescent Localization of VP7 Proteins in Transfected COS 7 Cells

The gene encoding the VP7 protein was inserted into the vector pJC119 under the control of the SV40 late promoter to generate the plasmid pJC9 (as described in the Materials and Methods). The expression of the VP7 protein from this gene was examined in transfected COS 7 cells to confirm the ER location of this protein. An indirect immunofluorescent procedure using a secondary fluorescein-coupled goat anti-rabbit Ig and a primary monospecific polyclonal rabbit antiserum was used to localize VP7. A concomitant display of WGA, conjugated to rhodamine (R-WGA), and known to specifically bind to sialic acid and terminal glucosamines in the Golgi apparatus (40), allowed us to determine if VP7 was present in this organelle. The immunolocalization of VP7 expressed from pJC9 shows a distinct, arborizing, reticular pattern of fluorescein staining radiating from the nucleus, and a perinuclear concentration of stained, reticular material (Fig.

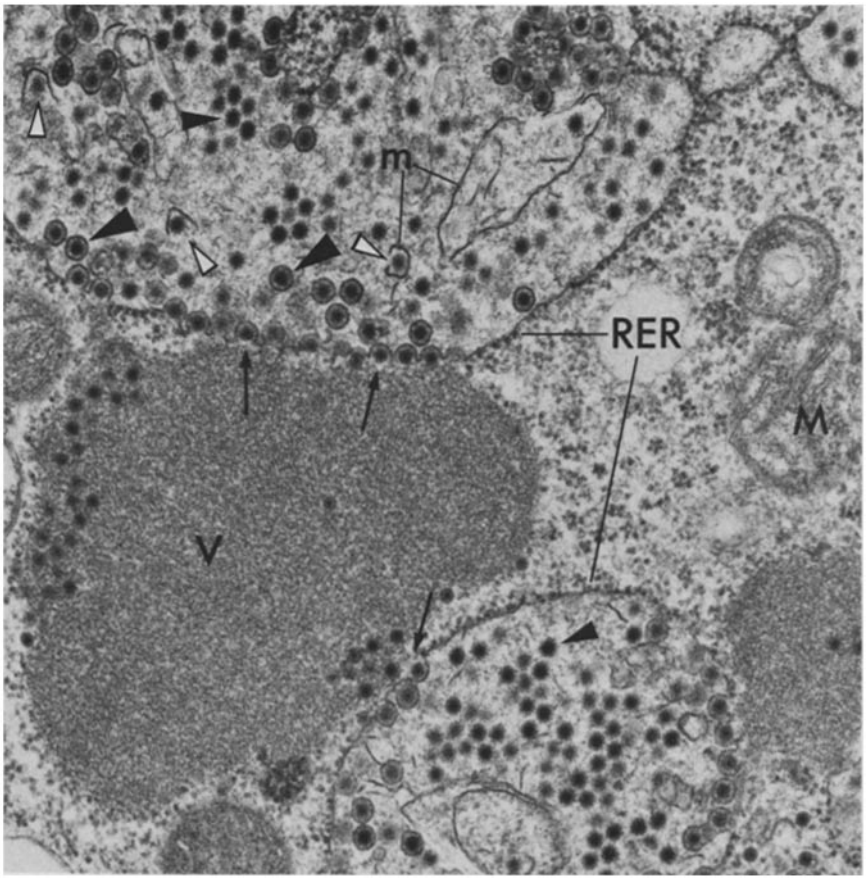

FIGURE 3 Morphology of SA11 rotavirus-infected MA104 cell at 5.5 h post-infection. Infected cells show spherical viroplasm (*V*) structures in the cytoplasm. These are composed of several viral proteins and nucleic acid which assemble into viral cores (arrows) that bud from the periphery of the viroplasm into the rough endoplasmic reticulum (*RER*). Immature viral particles with surrounding ER membrane appear in the lumen of the ER (large black arrowheads), as do numerous, non-enveloped, mature forms of the virion which are devoid of membrane (small black arrowheads). Several viral particles are indicated which apparently are in the process of losing the surrounding membrane (white arrowheads); possible membrane remnants can also be seen (*m*). M, mitochondrion. × 41,500.

5). This probably corresponds to the RER and to transitional elements of ER, spatially related to, but exclusive of, the Golgi apparatus (see Fig. 4*b* and *inset*). Nuclear staining is also evident. Fig. 5*b* shows the same cell stained with R-WGA. A staining pattern consisting of punctate material and a perinuclear localization, probably coincident with part of the Golgi apparatus and distinct from that of the VP7 localization, is seen. Thus, VP7 protein expressed from the wild-type gene in pJC9 appears to localize to the ER and does not appear to reach the Golgi apparatus.

A series of plasmids containing mutations in the VP7 gene has also been constructed (see Fig. 2). The deletions were constructed in order to study the role of the hydrophobic domains in VP7 synthesis. The location of VP7 expressed from these plasmids in COS 7 cells was also examined by immunofluorescence. The deletion mutant 1–14 displayed extensive ER and perinuclear staining in regions distinct from that seen for R-WGA (Fig. 5, *c* and *d*), similar to the wild-type. In this mutant, the first ATG codon was deleted so that only the second initiation codon and the hydrophobic region following it could be used (Fig. 2). Another mutant studied, 2–8, in which the sequence following the first ATG codon was modified (see Materials and Methods), showed results analogous to the wild-type (Fig. 5, *e* and *f*). In contrast, VP7 distribution in the mutants 42–61, 43–61, and 47–61, in which distal parts of the second hydrophobic domain were removed (Fig. 2), showed reticular staining and a distinct perinuclear distribution which coincided precisely with, or was a subset of, the R-WGA staining pattern (Fig. 5, *g–l*). Thus it appeared that with these deletions, the mutant VP7 proteins reached the Golgi apparatus. Mutant 51–61, whose deletion removed a region distal to the hydrophobic domains, exhibited a staining pattern identical to the wild-type, that of reticular staining and a perinuclear distribution distinct from that of the R-WGA staining pattern. It appears that the absence of the region coding for these amino acids was not sufficient to cause movement of VP7 out of the ER to the Golgi apparatus.

Intracellular Expression of VP7 Proteins

To confirm and extend the above results, we also examined VP7 expression from wild-type and mutant genes by immunoprecipitating radiolabeled proteins from cell lysates (see Materials and Methods). Cells were transfected with plasmids containing the wild-type gene (pJC9) or deletions 1–14, 2–8, 42–61, 43–61, 47–61, or 51–61 (Fig. 2). VP7 proteins were immunoprecipitated and displayed by gel electrophoresis before or after digestion with endo-H and compared on the same gel alongside L-[^{35}S]methionine-labeled SA11-infected MA104 cell lysate. No significant products were seen when either no DNA (Fig. 6) or the vector pJC119 was used as a control (see below, Fig. 8). However, the wild-type and mutant genes all expressed a protein(s) precipitable with anti-VP7 antiserum (Fig. 6, – lanes). In the case of the intact VP7 gene (pJC9) and the deletion 1–14, two products were seen in the absence of endo-H, but the lower band was relatively minor, not always reproducible, and its origin is uncertain. For mutants 42–61 and 51–61, two products were expressed and it is very likely that the lower molecular weight species was the nonglycosylated version of each protein. In the case of mutant 51–61, it is possible that the lower molecular weight band arises from use of the third in-frame AUG as a start

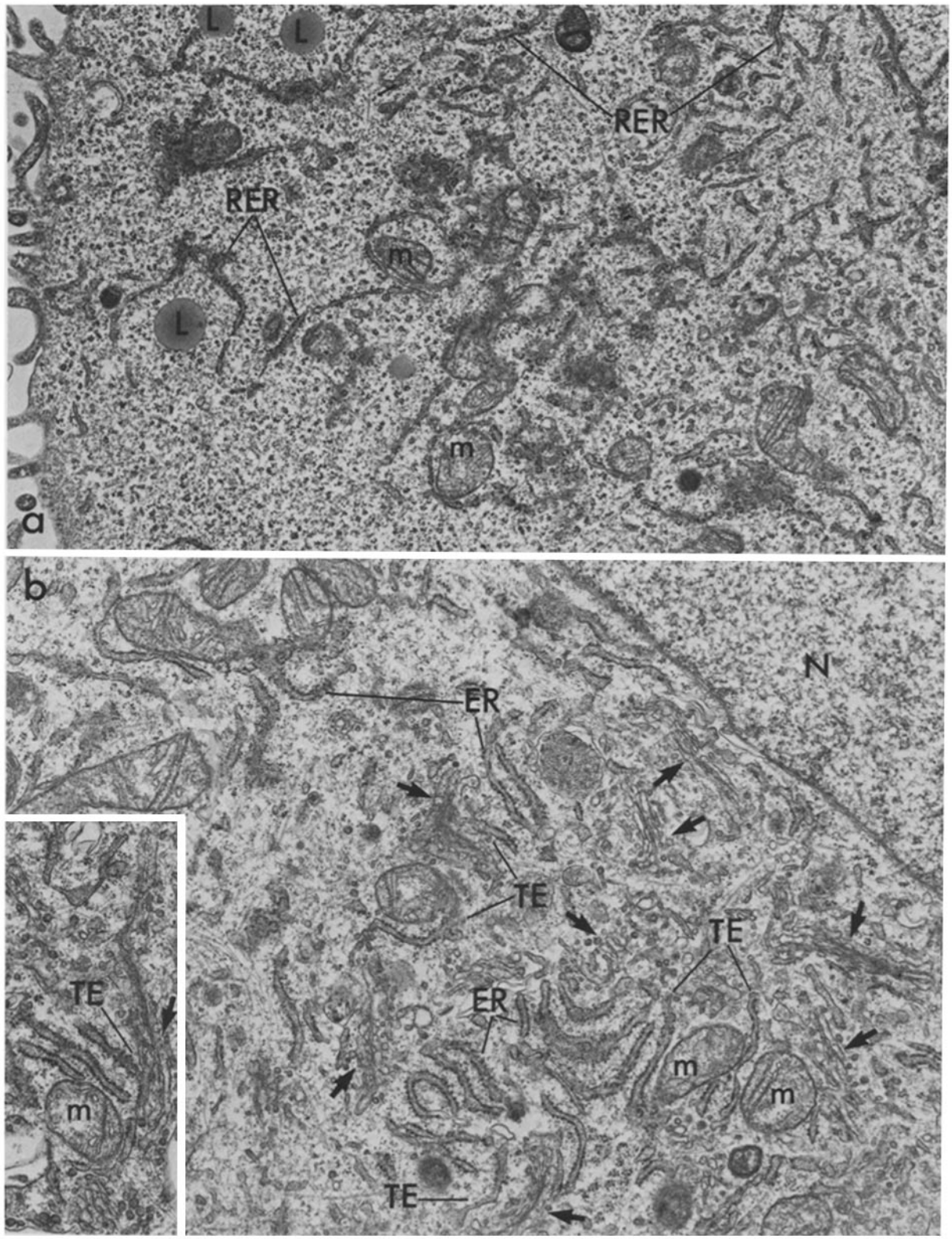

FIGURE 4 Morphology of peripheral and central regions of COS 7 cells. (*a*) The peripheral region of the cell is heavily populated with free polysomes. Mitochondria (*m*), lipid droplets (*L*), and portions of the rough endoplasmic reticulum (*RER*) extend into this region. The central regions of the cell are more densely populated with ER, transitional and smooth elements of ER. × 13,500. (*b* and *inset*) The perinuclear region of the COS 7 cell is typically characterized by an extensive Golgi apparatus. Its several stacks (arrows) are surrounded by extensive endoplasmic reticulum (ER) which exhibit ribosome-studded, transitional (*TE*), and smooth elements that spatially intertwine with, but are distinct from, the Golgi apparatus. *N*, nucleus; *m*, mitochondria. × 17,820. (*Inset*, 20,250.)

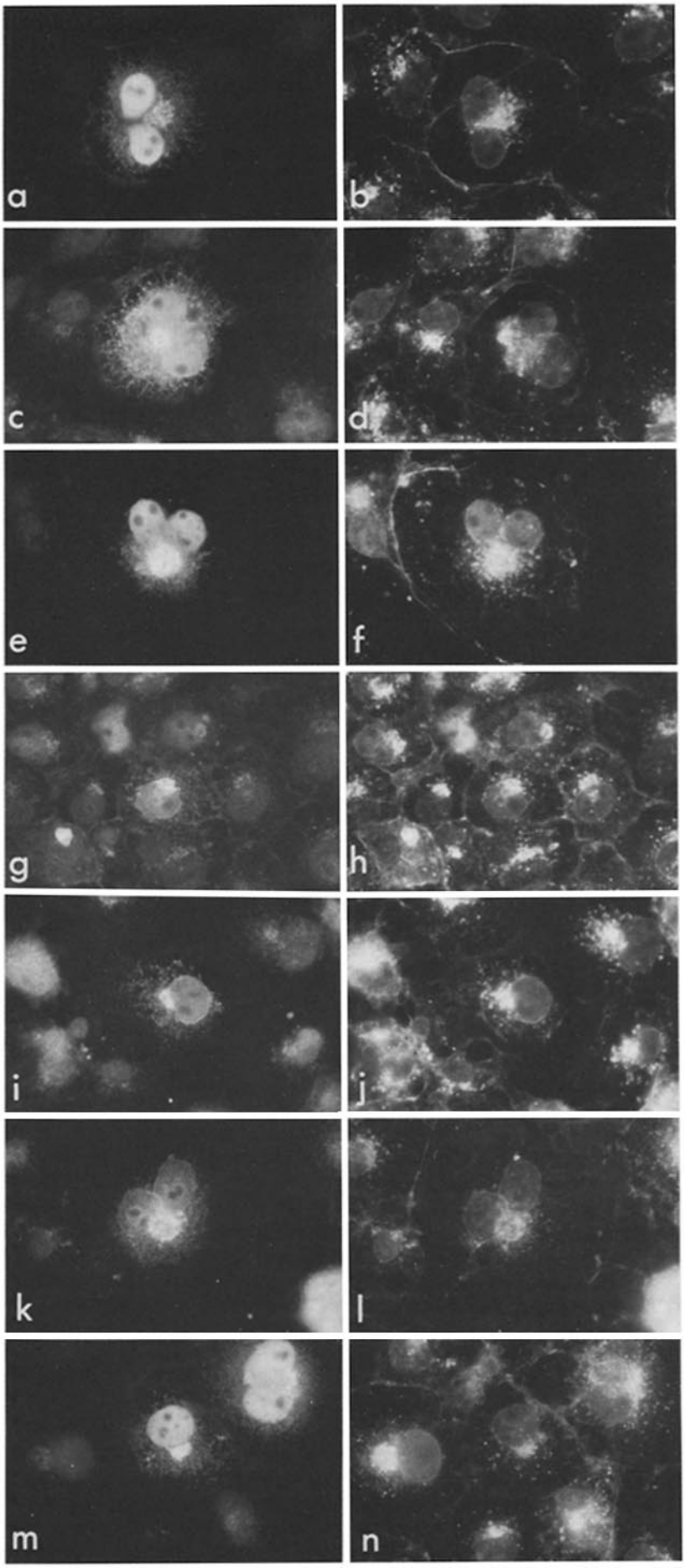

FIGURE 5 The immunofluorescent localization of VP7 (*left column*) compared with that of R-WGA (*right column*) in transfected COS 7 cells. Fluorescein coupled to goat anti-rabbit IgG was used secondary to primary rabbit polyclonal antiserum to immunolocalize VP7. All pairs were photographed in the same plane of focus. Cells transfected with pJC9 (*a* and *b*); mutants 1–14 (*c* and *d*); 2–8 (*e* and *f*); 42–61 (*g* and *h*); 43–61 (*i* and *j*); 47–61 (*k* and *l*); or 51–61 (*m* and *n*). VP7 is localized to an arborizing structure probably corresponding to ER, as well as to a perinuclear reticular structure, possibly transitional ER elements, which are distinct from but close to that of the perinuclear punctate stain for WGA and the Golgi apparatus as displayed in *a–f*, and *m* and *n*. In some cases, a negative image of the staining region of VP7 is seen for WGA (*c* and *d*). By contrast, the three deletions shown in *g–l* not only exhibit the ER reticular localization for VP7, but also a prominent perinuclear staining region that is precisely coincident with, or a subset of, the staining pattern for WGA. × 126.

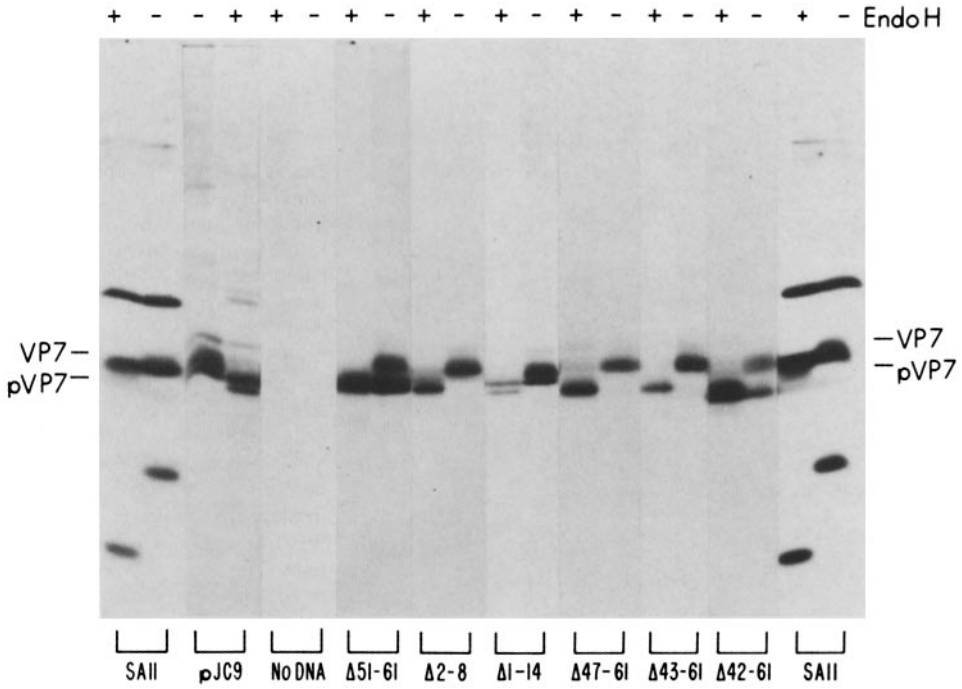

FIGURE 6 Endo-H sensitivity of intracellular products of cells transfected with full-length and mutated VP7 genes. Cells were labeled for 4 h with L-[^{35}S]methionine, as described in the text, the VP7 proteins immunoprecipitated (– lanes), and half of the samples digested with endo-H (+ lanes) (see Materials and Methods). Total SA11-infected MA104 cell lysate before (–) and after (+) Endo-H is shown as a marker to indicate the position of the glycosylated (VP7) and digested (pVP7) versions of VP7.

codon. This possibility is made less likely because for mutant 42–61 a similar unglycosylated band of the same size is secreted, implying the use of a functional signal which would not be translated if the third AUG was used as an initiation codon. The wild-type and mutant genes each expressed a product which was sensitive to endo-H (Fig. 6, + lanes), indicating that they were glycosylated with N-linked, high-mannose oligosaccharides. There was no significant intracellular pool of VP7 products that were resistant to endo-H (Fig. 6). Cells were transfected and then incubated in the presence or absence of tunicamycin and the resulting unglycosylated products were slightly smaller in size than those treated with endo-H (data not shown), again indicating the N-linked nature of the oligosaccharide. Taken together, these results imply that each mutant codes for proteins which retain a functional signal for translocation into the ER. For the 1–14 deletion, where only the second ATG and hydrophobic domain are retained, the latter probably constitutes the signal peptide. For the wild-type and other mutants, the translocation signal domain cannot be specified since both ATG codons and hydrophobic regions are present. Transfected cells labeled for 2.5 h showed an overall similar pattern of expression of the intracellular VP7 products, and again there was little evidence of intracellular material resistant to endo-H (data not shown).

Extracellular Products Expressed by VP7 Genes

Immunofluorescence studies indicated that for mutants 42–61, 43–61, and 47–61, VP7 staining co-localized with that of elements of the Golgi apparatus in COS 7 cells, indicating that these VP7 mutants were probably transported out of the ER. Therefore, the incubation media from all the transfected cell cultures described above were examined for secreted VP7 products. Three of the deletion mutants, 42–61, 43–61, and 47–61, affecting the distal region of the second hydrophobic domain produced VP7 molecules which were secreted (Fig. 7), in marked contrast to the behavior of the wild-type VP7 (pJC9), and the other mutants (51–61 in particular) (Fig. 7). The latter differed by only four amino acids from the secreted mutant 47–61 (Fig. 2). In addition, the secreted VP7 products were endo-H resistant (Fig. 7, + lanes), consistent with their passage through the Golgi apparatus and their modification to the complex type of carbohydrate. Densitometry of respective bands of original autoradiographs used for Figs. 6 and 7, which were equivalently exposed, showed that similar amounts of secreted and intracellular VP7 were present. These results pertain to cells labeled for 4 h. However, similar results were obtained in a 2.5-h labeling period (data not shown), indicating that secretion is an efficient process. The size of the VP7 which contained complex oligosaccharides (VP7^c) was slightly larger than that of VP7 with the high-mannose form of glycosylation (VP7) (Fig. 8, lanes *5* and *7*) as expected from the known higher molecular weight of complex N-linked oligosaccharides. Mutant 42–61 also secretes, based on its size, a nonglycosylated version of its mutant VP7 protein (Fig. 7). This was confirmed by another experiment where cultures transfected with mutants 42–61, 43–61, or 47–61 were subsequently treated with tunicamycin (Fig. 8, mutant 43–61 only shown). The product generated in the presence of tunicamycin (Fig. 8, + lanes) (VP7^u) is identical in size to the naturally occurring unglycosylated product of mutant 42–61 (Fig. 7). Some material the size of VP7 remained after tunicamycin treatment (Fig. 8, lane *8*) probably because of limiting amounts of the drug, since in other experiments tunicamycin resulted in complete conversion to VP7^u. In control cells, those not treated with tunicamycin (Fig. 8, lane *5*), the endo-H–resistant product was again secreted into the medium. Similar results were obtained with mutants 42–61 and 47–61 (data not shown). The amount of protein secreted in tunicamycin-treated cells (Fig. 8, lane *6*) was lower than that of the control, possibly because the drug interferes with secretion. No such bands were identified when the vector (pJC119), without VP7 gene insert, was used for transfection (Fig. 8, lanes *1–4*). The presence of prominent nonspecific background bands (Fig. 8, lanes *1*, *2*, *4*, and *6–8*), which are different for the intracellular (*intra*) and secreted (*sec*) lanes, does not alter this conclusion. These results confirm that the

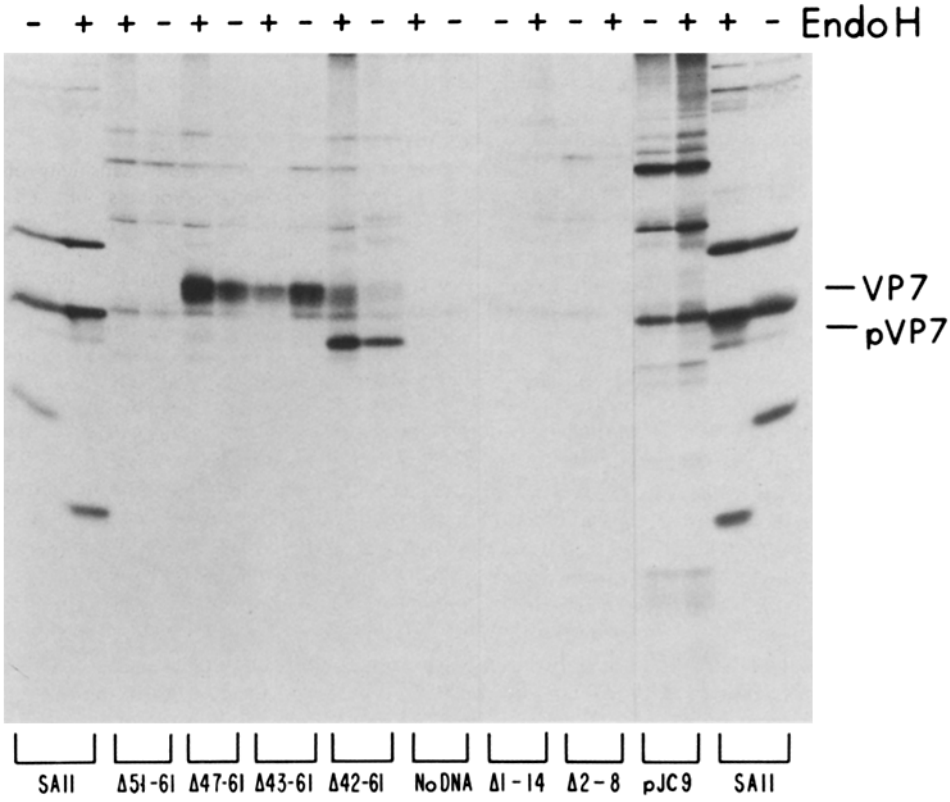

FIGURE 7 Endo-H sensitivity of immunoprecipitated products from the media of cells transfected with wild-type and mutated VP7 genes. Cells were labeled for 4 h with L-[^{35}S]methionine as described, the medium from each culture subjected to immunoprecipitation (− lanes), and half of the samples digested with endo-H (+ lanes). Total SA11-infected MA104 cell lysate before (−) and after (+) Endo-H displays marker glycosylated (VP7) and digested (pVP7) proteins. The length of exposure of this gel was equivalent to that of Fig. 6.

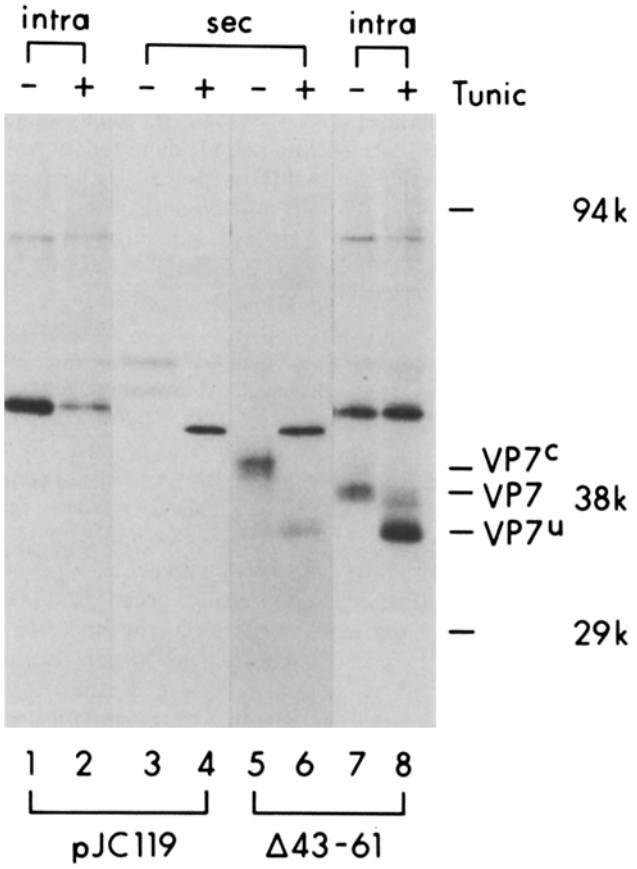

FIGURE 8 Secretion of mutant VP7 proteins in the presence of tunicamycin. Cells transfected with pJC119 (lanes *1–4*); or mutant 43-61 (lanes *5–8*), were labeled with L-[^{35}S]methionine for 4 h. Where indicated (+), tunicamycin (2 μg/ml) was added for the last 8 h of transfection; (−) are untreated cells. VP7^u refers to unglycosylated VP7 proteins, and VP7^c corresponds to VP7 with complex carbohydrate. The positions of migration in this gel of VP2 (*94k*), VP7 (*38k*) (with high-mannose carbohydrate), and NCVP5 (*29k*) in infected cell lysates are shown.

endo-H–resistant products secreted into the medium by these mutants contain an N-linked complex type of carbohydrate. Secreted VP7^c was again observed to be endo-H–resistant (data not shown) and to be present in approximately the same amount as the internal endo-H–sensitive VP7 (Fig. 8, lanes *5* and *7*).

DISCUSSION

In order to understand the specificity in the location of membrane glycoproteins, we have used a glycoprotein that is located in the ER in its natural state. ER location implies either the presence of a targeting signal specific for the ER or the absence of a positive signal that would otherwise direct the protein elsewhere. The structural glycoprotein VP7, of the rotavirus SA11, provides just such a naturally targeted ER protein. It is a membrane glycoprotein (21) before assembly into virus. How the transfer of the glycoprotein takes place is not known and we know of no other animal virus which exhibits this behavior. However, the mode of transfer of membrane protein to the virus particle resembles the assembly of coat protein into the filamentous phage M13 (44).

Analysis of the amino acid sequence of VP7 has shown the existence of two tandem NH_2-terminal hydrophobic domains, within the first 50 amino acids. Each is preceded by an in-frame ATG codon. Since the first ATG is "weak" and the second one has the preferred consensus sequence for initiation (24), we cannot be sure which one is used for VP7 synthesis, and are unable to say where the reported signal peptide cleavage occurs (13). Since mutant 1–14, which deletes the first ATG codon, still produces a glycoprotein located in the ER, the second hydrophobic domain can provide signal pep-

tide function. The NH_2-terminal hydrophobic domains seem important in the maturation of rotaviruses since the hydrophobic nature is highly conserved in the VP7 glycoproteins of viruses infecting human, simian, and bovine species (20), and therefore probably serve some role in anchoring this type of protein in the ER. There is no hydrophobic segment present at the COOH-terminus, a distinctive feature of the glycoproteins of plasma membrane maturing viruses. Our systematic generation of mutants affecting each or both of the hydrophobic regions was aimed at identifying the putative membrane anchor domain responsible for the ER location of the rotavirus VP7 glycoprotein.

The key observation is that in three of the deletion mutants extending into the second hydrophobic region, namely mutants 42–61, 43–61, and 47–61, the altered form of VP7 is secreted by transfected COS 7 cells and terminally glycosylated, a characteristic of a protein having traversed the normal secretory pathway. By contrast, neither the wild-type gene product was secreted, nor were products from deletions which affected other parts of the molecule. The deletion 1–14, which completely removed the first hydrophobic domain and mutant 2–8, in which the eight amino terminal residues conserved in all four rotavirus VP7 serotypes (9) were changed (see Materials and Methods), efficiently expressed glycoprotein located to the ER. Similarly, removal of only 11 amino acids downstream of the hydrophobic domains in mutant 51–61, apparently was not sufficient to influence the movement of VP7 from the ER to the Golgi apparatus. The only effect was to perturb the efficiency of glycosylation, perhaps for steric reasons, since the glycosylation site in the altered products is brought closer to the hydrophobic domains.

The carbohydrate present on VP7 is of the high-mannose type and is endo-H sensitive, consistent with its ER location and the absence of terminal processing of the oligosaccharide. Analysis of VP7 glycoprotein processing shows that it does not reach the Golgi apparatus but rather accumulates in a subcompartment of the ER in a processing pathway quite different from VSV G-protein (21). In our current observations, it should be noted that there is a distinctly larger size of the secreted VP7s in mutants 47–61, 43–61, and 42–61, due to the terminal glycosylation; they are also sensitive to tunicamycin and resistant to endo-H. This observation underscores the ER location of wild-type VP7 since it is apparent that its N-linked glycosylation can be modified and were the wild-type molecule to have reached the Golgi apparatus, further processing and terminal glycosylation should have occurred. In the mutant VP7s, the efficiency of secretion appears to be high for two reasons. First, there is no endo-H–resistant material inside the cell after either 2.5 or 4 h of labeling. Second, the amount of material secreted is similar in amount to that seen intracellularly.

Other glycoproteins of the ER have been cloned and some sequenced. In the cases of HMG-CoA reductase (27) and coronavirus E1 (4), there was no obvious homology between the NH_2-terminal hydrophobic domains in these molecules and VP7, nor with the dual NH_2-terminal hydrophobic domains in nonstructural rotavirus glycoprotein NCVP5 (8). Cytochrome P-450 (31), another ER protein, did not display any obvious homologies in its multiple hydrophobic domains. It should be noted, however, that 3-hydroxy-3-methylglutaryl-CoA reductase, coronavirus E1, and cytochrome P-450 probably interact with the lipid bilayer much more extensively than does VP7, via multiple membrane spanning domains.

Since VP7 is not normally secreted, presumably there could be no specific ER receptor (14, 28) mediating its secretion, and therefore its movement along the secretory pathway in these cells is constitutive, rather than specific. This is the first demonstration of an alteration in the primary sequence which allows a naturally targeted ER molecule to be secreted, and shows unequivocally that glycoproteins can be secreted without the intervention of a specific receptor. Also of significance is that an unglycosylated, mutant VP7 is efficiently secreted. The precise reason(s) for the secretion of VP7 in the mutants 42–61, 43–61, and 47–61 is not yet clear. It could be that an anchor region has been shortened so that it no longer functions, that a positive signal for ER location has been disrupted, or that a peptidase cleavage site, e.g., the Ala-Tyr-Ala sequence at residues 66–68 (43), has been brought into proximity of the aminopeptidase used for signal peptide cleavage. These possibilities are being investigated. Our results become particularly interesting when juxtaposed with several other observations. Firstly, some normally soluble molecules of the ER (2, 5) remain in the ER, whereas soluble VP7 is secreted. Secondly, influenza neuraminidase is anchored in the membrane by an NH_2-terminal hydrophobic domain, but this molecule, unlike VP7, is exported to the plasma membrane (6). From the above, we conclude that the region of the second hydrophobic domain of VP7 not only serves to anchor the protein in the membrane but may also contain the positive and specific signal for maintaining the protein in the ER.

We wish to thank Ms. Alisa Kabcenell for her critical review of the manuscript and Mr. George Dominguez for his skillful preparation of the final photographs.

This work was supported by grants from the United States Public Health Service, the National Institutes of Health (CA13402 awarded to P. H. Atkinson), Core Cancer Grant CA13330, and grants from the New Zealand Medical Research Council and the Diarrhoeal Diseases Control Programme of the World Health Organization awarded to A. R. Bellamy.

Received for publication 22 July 1985, and in revised form 21 August 1985.

Note Added in Proof: VP7 antigens secreted by COS 7 cells transfected with mutants 42–61, 43–61, or 47–61 were immunoprecipitable by polyclonal antiserum raised against intact SA11 virus illustrating that at least some epitopes on these molecules were in a native configuration.

REFERENCES

1. Altenburg, B. C., D. Y. Graham, and M. K. Estes. 1980. Ultrastructural study of rotavirus replication in cultured cells. *J. Gen. Virol.* 46:75–85.
2. Amar-Costesec, A., H. Beaufay, M. Wibo, D. Thines-Sempoux, E. Feytmans, M. Robbi, and J. Berthet. 1974. Analytical study of microsomes and isolated subcellular membranes from rat liver. II. Preparation and composition of the microsomal fraction. *J. Cell Biol.* 61:201–212.
3. Anderson, D. J., and G. Blobel. Immunoprecipitation of proteins from cell-free translations. Methods Enzymol. 96:111–120.
4. Armstrong, J., H. Niemann, S. Smeekens, P. Rottier, and G. Warren. 1984. Sequence and topology of a model intracellular membrane protein, E1 glycoprotein, from a coronavirus. *Nature (Lond.).* 308:751–752.
5. Beaufay, H., A. Amar-Costesec, D. Thines-Sempoux, M. Wibo, M. Robbi, and J. Berthet. 1974. Analytical study of microsomes and isolated subcellular membranes from rat liver. III. Subfractionation of the microsomal fraction by isopycnic and differential centrifugation in density gradients. *J. Cell Biol.* 61:213–231.
6. Bos, T. J., A. R. Davis, and D. P. Nayak. 1984. NH_2-terminal hydrophobic region of influenza virus neuraminidase provides the signal function in translocation. *Proc. Natl. Acad. Sci. USA.* 81:2327–2331.
7. Both, G. W., J. S. Mattick, and A. R. Bellamy. 1983. Serotype-specific glycoprotein of simian 11 rotavirus: coding assignment and gene sequence. *Proc. Natl. Acad. Sci. USA.* 80:3091–3095.
8. Both, G. W., L. J. Siegman, A. R. Bellamy, and P. H. Atkinson. 1983. Coding assignment and nucleotide sequence for Simian-11 rotavirus gene segment 10: location of glycosylation sites suggest that the signal peptide is not cleaved. *J. Virol.* 48:335–339.
9. Both, G. W., J. Mattick, L. Siegman, P. H. Atkinson, S. Weiss, A. R. Bellamy, J. E. Street, and P. Metcalf. 1983. Cloning of SA11 rotavirus genes: gene structure and

polypeptide assignment for the type-specific glycoprotein. *In* The Double-Stranded RNA Viruses. D. H. L. Bishop and R. W. Compans, editors. Elsevier Biomedical Press, New York. 73–82.
10. Chasey, D. 1980. Investigation of immunoperoxidase-labelled rotavirus in tissue culture by light and electron microscopy. *J. Gen. Virol.* 50:195–200.
11. Doyle, C., M. G. Roth, J. Sambrook, and M.-J. Gething. 1985. Mutations in the cytoplasmic domain of the influenza virus hemagglutinin affect different stages of intracellular transport. *J. Cell Biol.* 100:704–714.
12. Ericson, B. L., D. Y. Graham, B. B. Mason, and M. K. Estes. 1982. Identification, synthesis, and modifications of simian rotavirus SA11 polypeptides in infected cells. *J. Virol.* 42:825–839.
13. Ericson, B. L., D. Y. Graham, B. B. Mason, H. H. Hanssen, and M. K. Estes. 1983. Two types of glycoprotein precursors are produced by the simian rotavirus SA11. *Virology.* 127:320–332.
14. Fitting, T., and D. Kabat. 1982. Evidence for a glycoprotein "signal" involved in transport between subcellular organelles. *J. Biol. Chem.* 257:14011–14017.
15. Florkiewicz, R. Z., A. Smith, J. E. Bergmann, and J. K. Rose. 1983. Isolation of stable mouse cell lines that express cell surface and secreted forms of the vesicular stomatitis virus glycoprotein. *J. Cell Biol.* 97:1381–1388.
16. Garoff, H., C. Kondor-Koch, R. Pettersson, and B. Burke. 1983. Expression of Semliki Forest virus proteins from cloned complementary DNA. II. The membrane-spanning glycoprotein E2 is transported to the cell surface without its normal cytoplasmic domain. *J. Cell Biol.* 97:652–658.
17. Gething, M.-J., and J. Sambrook. 1982. Construction of influenza haemagglutinin genes that code for intracellular and secreted forms of the protein. *Nature (Lond.).* 300:598–603.
18. Gluzman, Y. 1981. SV40 transformed simian cells support the replication of early SV40 mutants. *Cell.* 23:177–182.
19. Guan, J-L., and J. K. Rose. 1984. Conversion of a secretory protein into a transmembrane protein results in its transport to the Golgi complex but not to the cell surface. *Cell.* 37:779–787.
20. Gunn, P. R., F. Sato, K. F. H. Powell, A. R. Bellamy, J. R. Napier, D. R. K. Harding, W. S. Hancock, L. J. Siegman, and G. W. Both. 1985. Rotavirus neutralizing protein VP7: antigenic determinants investigated by sequence analysis and peptide synthesis. *J. Virol.* 54:791–797.
21. Kabcenell, A. K., and P. H. Atkinson. 1985. Processing of the rough endoplasmic reticulum membrane glycoproteins of rotavirus SA11. *J. Cell Biol.* 101:1270–1280.
22. Klenk, H.-D., and R. Rott. 1980. Co-translational and post-translational processing of viral glycoproteins. *Curr. Top. Microbiol. Immunol.* 90:19–48.
23. Kondor-Koch, C., H. Riedel, K. Soderberg, and H. Garoff. 1982. Expression of the structural proteins of Semliki Forest virus from cloned cDNA microinjected into the nucleus of baby hamster kidney cells. *Proc. Natl. Acad. Sci. USA.* 79:4525–4529.
24. Kozak, M. 1983. Comparison of initiation of protein synthesis in procaryotes, eucaryotes and organelles. *Microbiol. Rev.* 47:1–45.
25. Laemmli, U. K. 1970. Cleavage of structural proteins during the assembly of the head of bacteriophage T4. *Nature (Lond.).* 227:680–685.
26. Langone, J. J. 1980. Radioiodination by use of the Bolton-Hunter and related reagents. *Methods Enzymol.* 70:221–247.
27. Liscum, L., J. Finer-Moore, R. M. Stroud, K. L. Lusakey, M. S. Brown, and J. L. Goldstein. 1985. Domain structure of 3-hydroxy-3-methylglutaryl coenzyme A reductase, a glycoprotein of the endoplasmic reticulum. *J. Biol. Chem.* 260:522–530.
28. Lodish, H. F., N. Kong, M. Snider, and G. J. A. M. Strous. 1983. Hepatoma secretory proteins migrate from rough endoplasmic reticulum to Golgi at characteristic rates. *Nature (Lond.).* 304:80–83.
29. Maniatis, T., E. Fritsch, and J. Sambrook. 1982. Molecular Cloning, A Laboratory Manual. Cold Spring Harbor Laboratory, New York. 545 pp.
30. Maxam, A. M., and W. Gilbert. 1977. A new method for sequencing DNA. *Proc. Natl. Acad. Sci. USA.* 74:560–564.
31. Ozols, J., F. S. Heinemann, and E. F. Johnson. 1985. The complete amino acid sequence of a constitutive form of liver microsomal cytochrome P-450. *J. Biol. Chem.* 260:5427–5434.
32. Petrie, B. L., D. Y. Graham, H. Hanssen, and M. K. Estes. 1982. Localization of rotavirus antigens in infected cells by ultrastructural immunocytochemistry. *J. Gen. Virol.* 63:457–467.
33. Reynolds, E. S. 1963. The use of lead citrate at high pH as an electron opaque stain in electron microscopy. *J. Cell Biol.* 17:208–212.
34. Rose, J., and J. E. Bergmann. 1982. Expression from cloned cDNA of cell-surface secreted forms of the glycoprotein of vesicular stomatitis virus in eucaryotic cells. *Cell.* 30:753–762.
35. Roth, M. G., R. W. Compans, L. Giusti, A. R. Davis, D. P. Nayak, M.-J. Gething, and J. Sambrook. 1983. Influenza virus hemagglutinin expression is polarized in cells infected with recombinant SV40 viruses carrying cloned hemagglutinin DNA. *Cell.* 33:435–443.
36. Sprague, J., J. H. Condra, H. Arnheiter, and R. A. Lazzarini. 1983. Expression of a recombinant DNA gene coding for the vesicular stomatitis virus nucleocapsid protein. *J. Virol.* 45:773–781.
37. Street, J. E., M. C. Croxson, W. F. Chadderton, and A. R. Bellamy. 1982. Sequence diversity of human rotavirus strains investigated by northern blot hybridization analysis. *J. Virol.* 43:369–378.
38. Sveda, M. M., L. J. Markoff, and C.-J. Lai. 1984. Influenza virus hemagglutinin containing an altered hydrophobic carboxy terminus accumulates intracellularly. *J. Virol.* 49:223–228.
39. Tarentino, A. L., and F. Maley. 1974. Purification and properties of an endo-β-*N*-acetylglucosaminidase from *Streptomyces griseus*. *J. Biol. Chem.* 249:811–817.
40. Tartakoff, A. M. 1983. The confined function model of the Golgi complex: center for ordered processing of biosynthetic products of the rough endoplasmic reticulum. *Int. Rev. Cytol.* 85:221–252.
41. Tkacz, J. S., and J. O. Lampen. 1975. Tunicamycin inhibition of polyisoprenyl *N*-acetylglucosaminyl pyrophosphate formation in calf liver microsomes. *Biochem. Biophys. Res. Commun.* 65:248–257.
42. Towbin, H., T. Staehelin, and J. Gordon. 1979. Electrophoretic transfer of proteins from polyacrylamide gels to nitrocellulose sheets: procedure and some applications. *Proc. Natl. Acad. Sci. USA.* 76:4350–4354.
43. Von Heijne, G. 1983. Patterns of amino acids near signal-sequence cleavage sites. *Eur. J. Biochem.* 133:17–21.
44. Webster, R. E., and J. S. Cashman. 1978. Morphogenesis of the filamentous single-stranded DNA phages. *In* The Single-Stranded DNA Phages. D. T. Denhardt, D. Dressler, and D. S. Ray, editors. Cold Spring Harbor Laboratory, New York. 557–569.
45. Wills, J. W., R. V. Srinivas, and E. Hunter. 1984. Mutations of the rous sarcoma virus *env* gene that affect the transport and subcellular location of the glycoprotein products. *J. Cell Biol.* 99:2011–2023.